

Structures in gas–liquid churn flow in a large diameter vertical pipe



Safa Sharaf, G. Peter van der Meulen¹, Ezekiel O. Agunlejika, Barry J. Azzopardi*

Faculty of Engineering, University of Nottingham, University Park, Nottingham NG7 2RD, UK

ARTICLE INFO

Article history:

Received 22 June 2015

Revised 12 September 2015

Accepted 12 September 2015

Available online 23 October 2015

Keywords:

Gas–liquid flow

Wire Mesh Sensor

Conductance probes

Churn flow

Vertical pipe

ABSTRACT

Gas–Liquid two phase co-current flow in a vertical riser with an internal diameter of 127 mm was investigated in the churn flow pattern. This paper presents detailed experimental data obtained using a Wire Mesh Sensor. It shows that the most obvious features of the flow are huge waves travelling on the liquid film. Wisps, large tendrils of liquid and the product of incomplete atomisation, which had previously detected in smaller diameter pipes, have also been found in the larger diameter pipe employed here. The output of the Wire Mesh Sensor has been used to determine the overall void fraction. When examined within a drift flux framework, it shows a distribution coefficient of ~ 1 , in contrast to data for lower gas flow rates. Film thickness time series extracted from the Wire Mesh Sensor output have been examined and the trends of mean film thickness, that of the base film and the wave peaks are presented and discussed. The occurrence of wisps and their frequencies have been quantified.

© 2015 The Authors. Published by Elsevier Ltd.

This is an open access article under the CC BY license (<http://creativecommons.org/licenses/by/4.0/>).

Introduction

Flow patterns in vertical pipes

Gas–liquid two-phase flow has many applications in the oil and gas, chemical and nuclear industries. When a two-phase mixture flows upwards in a vertical pipe, it is not possible to tell, a priori, how the phases are going to distribute themselves about the length and cross section of the pipe. Because of the infinite possibilities of distributions of the phases, researchers have tended to use flow patterns to describe the flows. These are broad descriptions of the flow. There is a consensus that the flow patterns for vertical flow are bubbly, slug, churn and annular. Some groups add other patterns such as wispy annular and dispersed bubble to this list. The identification of when each flow pattern occurs is difficult to determine. Direct observation through a transparent pipe section, particularly through a high speed camera, can allow visual and qualitative interpretation of the flow inside the pipe. However, this is very subjective, and in early projects such as by Bennett et al. (1965), researchers formed a consensus through anonymous voting. Visual observations are also problematic, because the flow at the pipe wall is often obscured by bubbles or waves on wall films, particularly at higher velocities, meaning that it is difficult to see what is happening deep inside the pipe through this approach alone. A more objective approach is to gather signals from instruments and then interpret those signals

quantitatively. What becomes obvious is that certain signatures are observed for particular types of flow, for example through the time series of void fraction and through the Probability Density Function (PDF). The PDF is a histogram of the occurrences of the different void fractions. This approach was used for example by Jones and Zuber (1975) and Costigan and Whalley (1997). For bubbly flow there is a single peak at low void fraction. Slug flow contains two peaks (1st peak–liquid slug, 2nd peak – large gas bubble). Churn flow occurs at void fractions above 0.5–0.6, and it has a single peak with a tail extending down to lower void fractions. Annular flow has a single narrow peak at high void fractions of usually greater than 0.8. Much of the published work to date concentrates on small diameter pipes from 10 to 50 mm. This is in contrast with the larger diameter pipes which are more common in industry (i.e., ≥ 75 mm).

As noted above the early study of Bennett et al. (1965) gave a strong indication of difficulty of identifying which flow patterns were present at particular flow rates. Their experiments were on steam/water at 35 and 70 bar in a 12.7 mm pipe. They presented their results as plots of mass flux versus quality (steam mass fraction). Subsequently, Hewitt and Roberts (1969), who carried out experiments with air/water in a 32 mm diameter pipe at 3 bar, showed that if plotted as the momentum fluxes (the product of density, ρ_i , times superficial velocity, u_{is} , squared, with $i = G$ for the gas and $= L$ for the liquid) for the two phases their own data and those of Bennett et al. (1965) showed that the different flow patterns were found grouped in particular parts of the plot. Two questions arise from this: why do the different data sets agree and why are dimensional groups being employed rather than the usual dimensionless ones? The answer to the first question is that the momentum flux (or inertia force) is one

* Corresponding author. Tel.: +44 115 951 4160; fax: +44 115 951 4115.

E-mail address: barry.azzopardi@nottingham.ac.uk (B.J. Azzopardi).

¹ Present address: Atlantic Drilling Services, Amsterdam, the Netherlands.

Table 1

Ratio of pipe diameter to surface tension for experiments of [Bennett et al. \(1965\)](#) and [Hewitt and Roberts \(1969\)](#).

Fluids	Pressure (bar)	Pipe diameter (mm)	Pipe diameter/surface tension (kg/ms ²)
Steam/water	35	12.7	0.45
Steam/water	70	12.7	0.72
Air/water	3	32	0.44

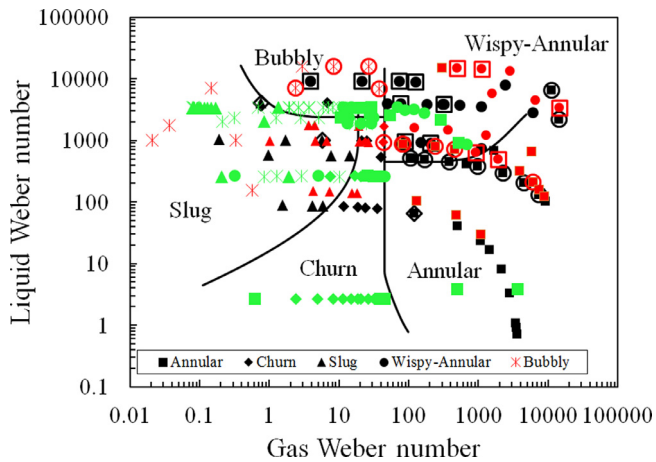


Fig. 1. Plot of liquid Weber number versus gas Weber number showing experimental flow pattern data of [Bennett et al. \(1965\)](#) (Steam/water – 12.7 mm diameter pipes – pressure 35 bar (Black symbols) and 70 bar (Red symbols)) and [Hewitt and Roberts \(1969\)](#) (Green symbols – air/water, 32 mm diameter pipe – pressure 4 bar) and transition lines adapted from [Hewitt and Roberts \(1969\)](#).

of the most important forces in determining flow pattern. The answer to why these dimensional plots work so well is probably due to the ratio of pipe diameter, D , to surface tension, σ , for the three different conditions studied. These are listed in [Table 1](#) where it can be seen that two of the values are almost identical and the third is close. This could explain the agreement between the different data sets. It points to a way of obtaining non-dimensional plots. If the momentum fluxes are multiplied by pipe diameter and divided by surface tension, the graph would be the same but with stretched axes. The combinations ($\rho_i u_i^2 D / \sigma$, where i is either gas or liquid) are Weber numbers, the ratio of inertial to surface tension forces. In much of gas/liquid flow with low viscosity liquids these are the most important forces. For example, in one of the most important phenomena which occurs in annular flows, the atomisation of drops from the wall film, it is a Weber number which controls the size and probably the flux of drops produced. In slug flow, the production of small bubbles from the tail of the large bubbles is similarly the balance of inertial and surface tension forces. The data from [Bennett et al. \(1965\)](#) and from [Hewitt and Roberts \(1969\)](#) have been replotted in terms of liquid and gas Weber numbers in [Fig. 1](#). Here the 35 bar steam–water data are plotted in black, the 70 bar steam–water data in red and the 3 bar air–water data in green. Where there was more than one flow pattern selected in the voting process, symbols for both patterns are plotted. There is some, but not strong, agreement with the boundaries between flow patterns suggested by [Hewitt and Roberts \(1969\)](#). This approach is for lower viscosity liquids. Obviously, a further refinement is required for more viscous liquids.

The fact that multiple flow patterns were selected for the same conditions might be taken as an indication of the difficulty of identifying the features of the flow from photographs taken through the transparent pipe wall but also through a wavy film on the wall or a layer of bubbles at the wall. However, it might also be evidence that the flow pattern transitions are not sharp but there is a gradual shift from the characteristics of one flow pattern to those of another with

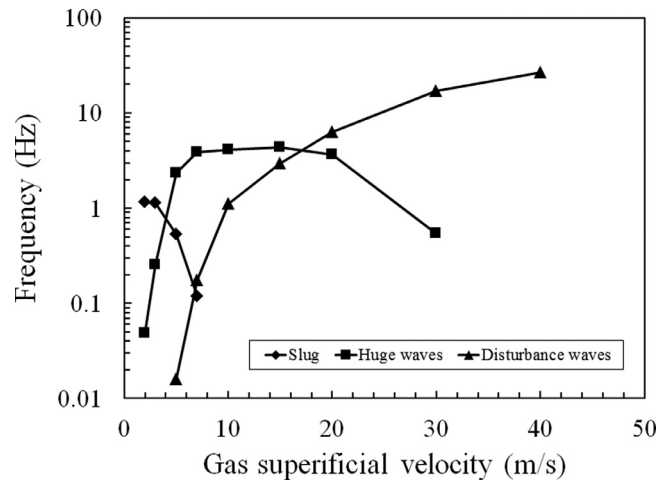


Fig. 2. Frequencies of slugs/huge waves/disturbance waves reported by [Sekoguchi and Mori \(1997\)](#). Pipe diameter = 25.8 mm, pressure = 2 bar, liquid superficial velocity = 0.4 m/s.

characteristics of both occurring simultaneously under some conditions. Further evidence of this gradual transition comes from the work of [Sekoguchi and Mori \(1997\)](#) who interrogated the gas–liquid flows using multiple probes, either axially or about a cross-section of the pipe. From the time resolved signals of all these probes they were able to identify individual examples of the structures which characterise each flow pattern. They found that more than one type of structure can occur at combinations of gas and liquid flow rates. [Fig. 2](#) illustrates the frequencies of the periodic structures that they obtained. The frequencies fall and rise systematically with increasing gas superficial velocity with regions where more than one structure is present. A similar plot, but for the lower superficial of 0.1 m/s was presented by [Hernandez Perez et al. \(2010\)](#).

Characteristics of individual flow patterns

Of the four major flow patterns, there is some consensus about the major mechanisms occurring in bubbly, slug and annular flows. *Bubbly* flow is recognised as consisting of bubbles dispersed in a liquid continuum. Recent work has noted the occurrence of waves of void fraction travelling up the pipe. [Taitel et al. \(1980\)](#) proposed that the transition to slug flow is based on the coalescence of bubble to form larger ones which eventually occupy the majority of the pipe cross-section and so become slug flow. The void fraction waves enhance the local bubble concentration at regular places along the pipe and encourage this coalescence process. It also explains why slugs occur regularly rather than randomly. *Slug* flow consists of alternate large, bullet-shaped bubbles (often called Demitrescu or Taylor bubbles) and liquid slugs containing small bubbles. There is creation of small bubbles from the tail of the Taylor bubbles with some of the newly created bubbles re-coalescing with the Taylor bubble whilst others passed deeper into the liquid slug. Models for slug flow have been proposed by [Fernandes et al. \(1983\)](#), [Sylvester \(1987\)](#), [deCachard and Delhaye \(1996\)](#) and [Brauner and Ullmann \(2004\)](#). Taylor bubbles have an obvious bullet shape separated by packets of liquid in smaller diameter pipes. Their velocities have a linear dependence on the mixture velocity (the sum of the superficial velocities of the gas and liquid) with a non-zero intercept, u_{ds} , which can be described by the rise velocity of an isolated Taylor bubble [$Fr \sqrt{(gD)}$] with g being the acceleration due to gravity. For the air–water combination at near atmospheric pressure, $Fr = 0.35$. For more viscous liquids, the equation proposed by [Viana et al. \(2003\)](#) has been found to be accurate for viscosities up to 360 Pa s. However, as the pipe diameter increases there is an increasing quantity of small bubbles in the liquid slugs and the shape of the Taylor bubble becomes more complex, losing its

Download English Version:

<https://daneshyari.com/en/article/7060310>

Download Persian Version:

<https://daneshyari.com/article/7060310>

[Daneshyari.com](https://daneshyari.com)